

Lineshape of $e^+e^- \rightarrow D^*\bar{D} + c.c.$ and electromagnetic form factor of $D^* \rightarrow D$ transition in the time-like region

Yuan-Jiang Zhang^{1*}, and Qiang Zhao^{1,2†}

1) *Institute of High Energy Physics, Chinese Academy of Sciences, Beijing 100049, P.R. China and*

2) *Theoretical Physics Center for Science Facilities, CAS, Beijing 100049, P.R. China*

(Dated: November 10, 2018)

In this work, we apply the vector meson dominance (VMD) model to extract the electromagnetic time-like form factor of the $D^* \rightarrow D$ transition combining the recent Belle data for $e^+e^- \rightarrow D^{*+}D^- + c.c.$ and data for $D^* \rightarrow D\gamma$. Two solutions are obtained in the interpretation of the cross section lineshape: i) With a relatively large coupling for $\psi D^*\bar{D}$ determined by experiment, destructive interferences among those charmonium components are required to bring down the overall cross sections, and then account for the cross section lineshape. ii) With a relatively small value for the $\psi D^*\bar{D}$ coupling based on heavy quark theory, an apparent cross section deficit near threshold is observed, and contributions from other mechanisms are needed. It might imply the presence of an additional resonance $X(3900)$. Meanwhile, we also point out that an enhancement like that could be produced by the $D_s^*\bar{D}_s + c.c.$ open channel effects.

PACS numbers: 12.40.Vv, 13.40.Gp, 13.66.Bc

I. INTRODUCTION

The $D\bar{D}^* + c.c.$ productions in e^+e^- annihilation give access to the study of the time-like electromagnetic (EM) form factor of $D^* \rightarrow D\gamma^*$ transition in the charmonium mass region. Their cross sections were measured recently by Belle [1] and BABAR [2], and clear resonance structures were observed above the $D\bar{D}^*$ or $D^*\bar{D}$ threshold. In the real photon limit, the coupling form factor can be measured via $D^* \rightarrow D\gamma$, which turns out to be an important decay mode for both the charged and neutral D^* mesons [3]. In particular, it shows that the partial decay coupling for $D^{*0} \rightarrow D^0\gamma$ could be much larger than that for $D^{*\pm} \rightarrow D^\pm\gamma$. This feature initiated a lot of efforts on understanding the $D^* \rightarrow D$ transition form factor.

Our motivation in this work is to study the $D^* \rightarrow D\gamma^*$ form factor in the time-like region with the help of the recent experimental data [1, 2]. We shall take into account the resonance contributions to the form factor by employing the extended vector meson dominance (VMD) model [4, 5]. To connect the real photon limit to the energy region above the $D^*\bar{D}$ threshold, we also include the light vector meson contributions. In Ref. [6], a VMD model was adopted for studying the $D^* \rightarrow D\gamma^*$ form factor. However, due to lack of experimental information at that time, the authors assumed that the widths for all vector mesons apart from the $\psi(4040)$ (and beyond) are zero. This should be a too-rough approximation. As studied recently in Ref. [7], the width effects were found essentially important for understanding the cross section lineshape of $e^+e^- \rightarrow D\bar{D}$.

Another useful and correlated channel is $D^* \rightarrow De^+e^-$, which probes the time-like form factor in small momentum squared region. However, due to the significant suppression of the EM vertex, branching ratio of this channel is expected to be very small and hard to measure. This branching ratio can be calculated in our model and serves as a prediction from theory.

There is a great advantage for extracting the $D^* \rightarrow D\gamma^*$ form factor in $e^+e^- \rightarrow D^*\bar{D} + c.c.$ Namely, there is only one Lorentz structure for the VVP coupling, where V and P stand for vector and pseudoscalar meson fields, respectively. Therefore, all information about the transition mechanisms would

* E-mail: yjzhang@ihep.ac.cn

† E-mail: zhaoq@ihep.ac.cn

be contained in a single coupling form factor, which is a complex function of the photon's four-vector momentum squared. Our calculations will be compared with the Belle data for $e^+e^- \rightarrow D^+D^{*-} + c.c.$ [1].

As follows, we first present the details of the VMD model in Sec. II. The numerical results will be given in Sec. III. Section IV is devoted to a summary and discussion.

II. THE MODEL

The typical effective Lagrangian for the $\gamma^*D^*\bar{D}$ and $\gamma^*\bar{D}^*D$ coupling can be written as:

$$\mathcal{L} = -ieg_{\gamma^*D^*\bar{D}}\varepsilon_{\alpha\beta\mu\nu}\partial^\alpha A^\beta\partial^\mu D^{*\nu}\bar{D} + h.c., \quad (1)$$

where A^β is the vector meson and electromagnetic field, $\varepsilon_{\alpha\beta\mu\nu}$ is the antisymmetric tensor. With Eq. (1), the matrix element of $e^+e^- \rightarrow D^*\bar{D}$ in the one-photon approximation can be written as:

$$T = e^2\bar{v}(k_2)\gamma_\alpha u(k_1)\frac{1}{s}g_{\gamma^*D^*\bar{D}}(s)\varepsilon_{\alpha\beta\mu\nu}p_{\bar{D}}^\beta p_{D^*}^\mu \epsilon^\nu, \quad (2)$$

where $u(k_1)$ and $v(k_2)$ are the Dirac spinors of the electron and positron, respectively; ϵ^ν represents the D^* -meson polarization vector, and $g_{\gamma^*D^*\bar{D}}(s)$ is the effective coupling form factor for the $D^* \rightarrow D$ transition. Note that the electron charge e has been isolated out in this definition. In the above equation, $s = (k_1 + k_2)^2$ is the overall center mass energy, while $p_{\bar{D}}$ and p_{D^*} are the four-vector momenta of the final state \bar{D} and D^* meson.

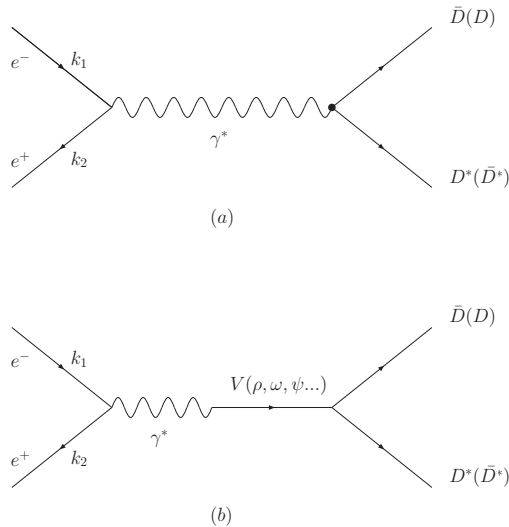


FIG. 1: Schematic diagrams based on the VMD model for $e^+e^- \rightarrow D^*\bar{D} + c.c.$ Diagram (a) is for the single photon approximation with an effective coupling $g_{\gamma^*D^*\bar{D}}(s)$, while (b) represents that the electromagnetic field is decomposed into the sum of vector meson fields.

As shown in Fig. 1, with the VMD model [4, 5] we can decompose the electromagnetic current into a sum of all vector meson fields including both isospin-0 and isospin-1 components. The $V\gamma^*$ effective coupling can be written as:

$$\mathcal{L}_{V\gamma} = \sum_V \frac{eM_V^2}{f_V} V_\mu A^\mu, \quad (3)$$

where $V^\mu (= \rho, \omega, \phi, J/\psi\dots)$ is the vector meson field, and eM_V^2/f_V is the photon-vector-meson coupling

TABLE I: Resonance parameters of the vector mesons adopted in this study. They are taken from PDG [3].

	$\rho(770)$	$\rho(1450)$	$\rho(1700)$	$\omega(782)$	$\omega(1420)$	$\omega(1680)$	J/ψ	$\psi(3686)$	$\psi(3770)$	$\psi(4040)$
M_V (GeV)	0.774	1.465	1.720	0.783	1.45	1.62	3.097	3.686	3.773	4.039
Γ_V (MeV)	149.4	400.0	250.0	8.5	200.0	250.0	9.32×10^{-2}	0.317	27.3	80
Γ_{ee} (keV)	7.04	-	-	0.6	0.46	0.8	5.55	2.38	0.265	0.86

constant. Setting $m_e \simeq 0$, e/f_V can be extracted from the partial decay width $\Gamma_{V \rightarrow e^+e^-}$ by:

$$\frac{e}{f_V} = \left[\frac{3\Gamma_{V \rightarrow e^+e^-}}{2\alpha_e |\vec{p}_e|} \right]^{\frac{1}{2}}, \quad (4)$$

where $|\vec{p}_e|$ is the electron three-vector momentum in the vector meson rest frame, and α_e is the fine-structure constant.

The following effective Lagrangians are required for vector meson couplings to the D meson pair and $D^* \bar{D}$:

$$\begin{aligned} \mathcal{L}_{VD\bar{D}} &= g_{VD\bar{D}} \{D \partial_\mu \bar{D} - \partial_\mu D \bar{D}\} V^\mu, \\ \mathcal{L}_{VD^*\bar{D}} &= -i g_{VD^*\bar{D}} \varepsilon_{\alpha\beta\mu\nu} \partial^\alpha V^\beta \partial^\mu D^{*\nu} \bar{D} + h.c. \end{aligned} \quad (5)$$

The effective coupling $g_{\gamma^* D^* \bar{D}}(s)$ can then be expressed in a general form:

$$g_{\gamma^* D^* \bar{D}}(s) = \sum_V \frac{M_V^2}{f_V} \frac{1}{s - M_V^2 + i\sqrt{s} \Gamma_V} g_{VD^*\bar{D}}, \quad (6)$$

where Γ_V is the total decay width of the vector meson. The total cross section for $e^+e^- \rightarrow D^{*+}D^- + c.c.$ thus reads

$$\sigma(e^+e^- \rightarrow D^{*+}D^- + c.c.) = \frac{8\pi}{3} \frac{|\vec{p}|^3}{s^{3/2}} \alpha_e^2 \left| \sum_V \frac{M_V^2}{f_V} \frac{g_{VD^*\bar{D}}}{s - M_V^2 + i\sqrt{s} \Gamma_V} \right|^2. \quad (7)$$

where $g_{VD^*\bar{D}} \equiv g_{VD^{*+}D^-} = g_{VD^{*-}D^+}$. In this paper, our definition for $g_{VD^*\bar{D}}$ is different from that in Ref. [7]. Namely, it does not include the charge conjugate coupling. In Ref. [7], $g_{VD^*\bar{D}} \equiv \sqrt{2}g_{VD^{*+}D^-} = \sqrt{2}g_{VD^{*-}D^+}$. Thus, Eq. (7) has a factor of 2 different from Eq. (12) in Ref. [7].

In the following calculation, we mainly consider the contributions from ρ , ω , J/ψ , and their radial excitation states. the contributions from the ϕ -mesons are dropped because the $g_{\phi D^* \bar{D}}$ couplings are strongly suppressed by the Okubo-Zweig-Iizuka (OZI) rule. The $g_{\Upsilon D^* \bar{D}}$ couplings are also suppressed by the OZI rule. Moreover, the Υ states are far away from the $D^* \bar{D}$ threshold. Thus, their contributions can be safely neglected. Parameters for the vector mesons are listed in Table I.

The asymptotic behavior of $g_{\gamma^* D^* \bar{D}}(s)$ has been discussed in Ref. [6]. As $s \rightarrow \infty$, form factor $g_{\gamma^* D^* \bar{D}}(s)$ must decrease at least as s^{-2} to avoid the violation of unitarity. As a consequence, the following relations are obtained for the isospin-1 and the isospin-0 components:

$$\sum_{\rho_i} \frac{M_{\rho_i}^2}{f_{\rho_i}} g_{\rho_i D^* \bar{D}} = 0, \quad (8)$$

and

$$\sum_{V(I=0)} \frac{M_{V(I=0)}^2}{f_{V(I=0)}} g_{V(I=0) D^* \bar{D}} = 0. \quad (9)$$

As discussed in Ref. [6], the above asymptotic relation implies that at least two ρ mesons are needed in the VMD model.

We also adopt the following relations given by the SU(3) quark model:

$$f_{\omega_i} \simeq 3f_{\rho_i}, \quad m_{\rho_i}^2 \simeq m_{\omega_i}^2, \quad (10)$$

where the factor 3 can be tested well by the partial decay widths for ω_i and ρ_i via Eq. (4). With the flavor symmetry, we also have:

$$g_{\omega_i D^{*+} D^-} = -g_{\rho_i D^{*+} D^-}. \quad (11)$$

It is worth noting that the above relations, i.e. Eqs. (8), (10) and (11), imply a negligible contribution from the ρ and ω mesons in the production of $D^* \bar{D} + c.c.$ pairs in $e^+ e^-$ annihilation, although they are dominant in the D^* radiative decays.

The strong coupling $g_{V D^* \bar{D}}$ for those charmonium states below the $D^* \bar{D}$ threshold cannot be directly extracted from the experimental data, such as $g_{J/\psi D^* \bar{D}}$. Their coupling values generally have large discrepancies in different models. The relation between $g_{V D^* \bar{D}}$ and $g_{V D \bar{D}}$ can be parameterized by:

$$g_{V D^* \bar{D}} = g_{V D \bar{D}} \times g_V, \quad (12)$$

where g_V is a parameter with inverse of mass dimension. In the heavy quark mass limit [8], one has $g_V = 1/\sqrt{m_{D^*} m_D} \simeq 0.52 \text{ GeV}^{-1}$. In contrast, the relativistic potential model of Ref. [9] gives:

$$g_V = \frac{e_Q}{\Lambda_Q} + \frac{e_q}{\Lambda_q}, \quad (13)$$

where e_Q is the heavy quark charge and e_q is the light quark charges, and the expressions of Λ_Q and Λ_q can be found in Ref. [9]. It should be mentioned that as pointed out in Ref. [10], Equation (13) is a general consequence of decomposing the electromagnetic current into a heavy and light part in the radiative decay $D^* \rightarrow D\gamma$. In Ref. [11], the value $g_{J/\psi} \sim 1.0 \text{ GeV}^{-1}$ is extracted, and QCD sum rules give $g_{J/\psi} = 0.69 \pm 0.14 \text{ GeV}^{-1}$ [12].

In the numerical calculation, we neglect the coupling differences between the charge and neutral channels for $g_{V D^* \bar{D}}$ and $g_{V D \bar{D}}$. The coupling constants $g_{\psi' D \bar{D}}$ and $g_{\psi(3770) D \bar{D}}$ have been discussed in our previous work [7], and $g_{\psi(3770) D \bar{D}} \simeq 12.7$ is extracted from the experimental result [3] by the effective Lagrangian approach. The coupling $g_{\psi' D \bar{D}} \simeq 9.05$ is determined by fitting the lineshape of $e^+ e^- \rightarrow D \bar{D}$ process. We adopt $g_{J/\psi D \bar{D}} = 7.44$ from Ref. [13], which is obtained by the VMD model.

We must note that the cross section measurement gives access to the absolute value of $|g_{\gamma^* D^* \bar{D}}(s)|$. But $g_{\gamma^* D^* \bar{D}}(s)$ is a complex function of s in the time-like region. Moreover, the prescription at the hadronic level will introduce a phase factor $e^{i\phi}$ to each resonance amplitude. These phase angles, apart from an overall phase, can be determined by fitting the Belle data for $e^+ e^- \rightarrow D^{*+} D^- + c.c.$ [1].

As one can see that the Belle data cover a rather high \sqrt{s} region, it is natural to anticipate that the low \sqrt{s} form factor would be less sensitive to the data constraints. Taking into account this, we include the real photon data for $D^* \rightarrow D\gamma$ in the numerical fitting. In the real photon limit, it is rather direct to obtain the partial width of $D^* \rightarrow D\gamma$ by

$$\Gamma(D^* \rightarrow D\gamma) = \frac{\alpha_e}{3} g_{\gamma^* D^* D}^2(0) q^3, \quad (14)$$

where q is the photon energy in the D^* rest frame. Again, $g_{\gamma^* D^* D}(0)$ can be expressed as Eq. (6). This would provide constraints on the parameters from light vector meson components.

The decay of $D^* \rightarrow D e^+ e^-$ also gives access to the transition form factor at low \sqrt{s} . The matrix element of the $D^* \rightarrow D e^+ e^-$ decay via single photon transition can be written as

$$T = g_{\gamma^* D^* \bar{D}}(k^2) \frac{e^2}{k^2} \varepsilon_{\alpha\beta\mu\nu} p_D^\beta p_{D^*}^\mu \epsilon^\nu \bar{u}(k_1) \gamma_\alpha v(k_2), \quad (15)$$

where k^2 is the invariant mass of the lepton pair. The formula of the differential probability can be described by the following expression:

$$\frac{d\Gamma}{dk^2 dQ^2} = \frac{\alpha_e^2 |g_{\gamma^* D^* \bar{D}}(k^2)|^2}{48\pi m_{D^*}^3} [k^2 + 2Q^2 - 2m_D^2 - 2m_{D^*}^2]$$

$$\begin{aligned}
& + \frac{(m_{D^*}^2 - m_e^2 - Q^2)^2 + (m_D^2 - m_e^2 - Q^2)^2 - 8m_e^2 Q^2}{k^2} \\
& + \frac{2(m_{D^*}^2 - m_D^2)^2 m_e^2}{k^4} \Big], \tag{16}
\end{aligned}$$

where Q^2 is defined as $Q^2 = (k_2 + p_D)^2$ (or $Q^2 = (k_1 + p_D)^2$). We should note that this process is strongly suppressed by an additional EM coupling in respect of $D^* \rightarrow D\gamma$. Therefore, it is relatively difficult to measure this branching ratio in experiment.

III. NUMERICAL RESULTS

Now, we switch to the details of the numerical fitting. First, we give a brief discussion about the fitting scheme:

(i) Since only the relative phase can be measured in experiment, we set $\phi_{J/\psi} = 0^\circ$, and then the other phase angles are defined in respect of $\phi_{J/\psi}$. Meanwhile, since the cross sections are not sensitive to the light vector meson contributions, the relative phases ϕ_{ρ_i} and ϕ_{ω_i} are set the same and denoted by ϕ_{LV} in the fitting.

(ii) As shown by the cross sections around 4.2 GeV, there is no clear evidence for an enhancement due to the presence of a resonance. Therefore, the data for $e^+e^- \rightarrow D^*\bar{D} + c.c.$ cannot constrain $\phi_{Y(4260)}$ at all. For simplicity, we set $\phi_{Y(4260)} = 0^\circ$.

(iii) For $\psi(4040)$ and $Y(4260)$, $g_{VD^*\bar{D}}$ are not clear. Especially, the $\frac{M_V^2}{f_V}$ for $Y(4260)$ is also unavailable. In the numerical fitting, these two couplings are always combined. Thus, we define $g_V^{\text{eff}} \equiv \frac{M_V^2}{f_V} \times g_{VD^*\bar{D}}$ for $\psi(4040)$ and $Y(4260)$. In total, the fitting parameters include the relative phases ϕ_{LV} , $\phi_{\psi'}$, $\phi_{\psi(3770)}$, $\phi_{\psi(4040)}$, and the couplings $g_{\psi(4040)}^{\text{eff}}$ and $g_{\psi(4260)}^{\text{eff}}$.

As discussed previously, the charmed meson couplings to the light mesons are obtained in the chiral and heavy quark limits [14]: $g_{\rho_i D^* D} = \sqrt{2}\lambda m_{\rho_i} / f_\pi$, with $f_\pi = 132$ MeV, and $\lambda = 0.56$ GeV $^{-1}$ [15]. These couplings contain uncertainties arising from g_V as illustrated by Eq. (13). Also, since the constraints on the light vector mesons are rather weak in the data for $e^+e^- \rightarrow D^*\bar{D} + c.c.$, we thus include the data for $D^* \rightarrow D\gamma$ to constrain couplings g_ρ and g_ω .

For charmonium coupling to the charmed mesons, the following relation is assumed:

$$g_\psi \equiv g_{J/\psi} \simeq g_{\psi'} \simeq g_{\psi(3770)} \simeq g_{\psi(4040)}, \tag{17}$$

which can be determined by

$$\frac{\Gamma(\psi(4040) \rightarrow D\bar{D})}{\Gamma(\psi(4040) \rightarrow D^*\bar{D} + c.c.)} = \frac{|\vec{p}_1|^3}{g_\psi^2 M_{\psi(4040)}^2 |\vec{p}_2|^3}, \tag{18}$$

where \vec{p}_1 and \vec{p}_2 are the three momenta of the final charmed mesons in $\psi(4040) \rightarrow D\bar{D}$ and $\psi(4040) \rightarrow D^*\bar{D} + c.c.$, respectively. Hence, given the experimental data [3],

$$\frac{\Gamma(\psi(4040) \rightarrow D^0\bar{D}^0)}{\Gamma(\psi(4040) \rightarrow D^{*0}\bar{D}^0 + c.c.)} = 0.05 \pm 0.03, \tag{19}$$

we have $g_\psi = 1.73 \pm 0.52$ GeV $^{-1}$ by taking the average value corresponding to the datum bound. This value appears to be larger than $g_V \simeq 0.52$ GeV $^{-1}$ extracted by Ref. [8] and $g_V \sim 1.0$ GeV $^{-1}$ by Ref. [11]. In order to examine the impact of the uncertainties due to g_V , we shall fix $g_\psi = 1.73$ GeV $^{-1}$ and 0.52 GeV $^{-1}$, respectively, in the numerical fitting.

A. With relatively large g_ψ determined by experimental data

In Table II, all the fitted parameters are listed. It shows that the coupling $g_{Y(4260)}^{\text{eff}}$ has a large uncertainty, which reflects the negligible role played by $Y(4260)$ in the fitting. Further experimental data with high accuracy are needed to extract its resonance parameters.

TABLE II: Model parameters obtained from the χ^2 minimization fitting with $g_\psi = 1.73 \text{ GeV}^{-1}$. Coupling g_V^{eff} is defined by $g_V^{\text{eff}} \equiv \frac{M_V^2}{f_V} \times g_{VD^*\bar{D}}$. The phase angles are in radian. The reduced χ^2 is $\chi^2/\text{d.o.f} = 41.2/51$.

parameter	ϕ_{LV}	$\phi_{\psi'}$	$\phi_{\psi(3770)}$	$\phi_{\psi(4040)}$	$g_{\psi(4040)}^{\text{eff}}$	$g_{Y(4260)}^{\text{eff}}$
	-0.41 ± 0.17	2.36 ± 0.32	4.54 ± 0.22	-0.68 ± 0.21	0.37 ± 0.05	0.02 ± 0.03

With the help of Eq. (4) and the fitted value for $g_{\psi(4040)}^{\text{eff}}$, we obtain $g_{\psi(4040)D^*\bar{D}} = 0.74 \pm 0.1 \text{ GeV}^{-1}$. Consequently, the partial decay width of $\psi(4040) \rightarrow D^*\bar{D} + c.c.$ can be accessed:

$$\begin{aligned} \Gamma(\psi(4040) \rightarrow D^{*+}D^- + c.c.) &= 5.1 \pm 1.0 \text{ MeV}, \\ \Gamma(\psi(4040) \rightarrow D^{*0}\bar{D}^0 + c.c.) &= 5.5 \pm 1.1 \text{ MeV}. \end{aligned} \quad (20)$$

An interesting result from this fitting is that, although $g_{VD^*\bar{D}}$ bares large uncertainties, the excitations of the charmonium states J/ψ , ψ' , and $\psi(3770)$, and their interferences play a major role on the interpretation of the effective coupling $g_{\gamma^*D^*\bar{D}}$ or $g_{\gamma^*D\bar{D}}$ [7]. This feature can be seen more clearly via the fitted cross sections.

In Fig. 2(a), the total cross section and cross sections for exclusive resonances are plotted. We do not show the curve of $Y(4260)$ since its contribution is negligibly small. Interestingly, other charmonia, such as J/ψ , ψ' , and $\psi(3770)$, have large exclusive cross sections. In particular, the cross section for the ψ' excitation over-shoots the data apparently, and cancellations among these three amplitudes are required to reproduce the lineshape of the cross sections.

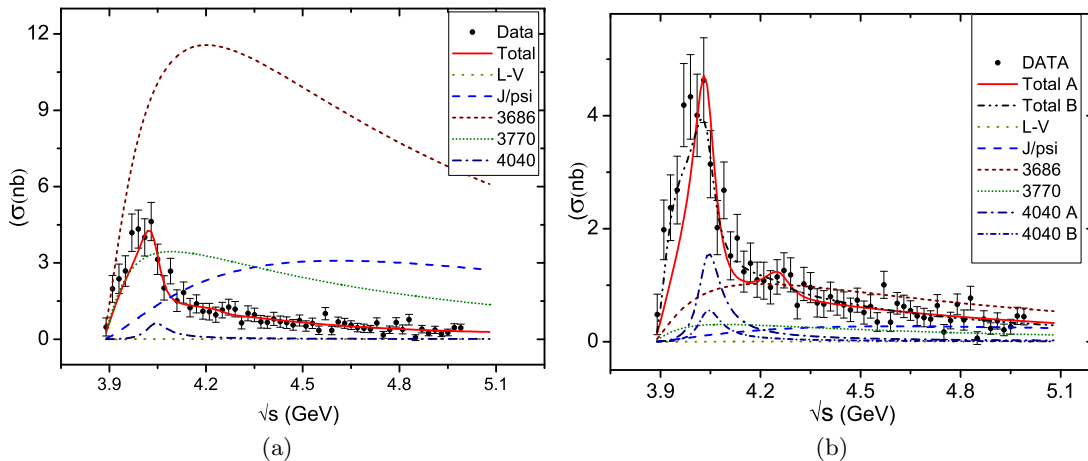


FIG. 2: The Belle data for the $e^+e^- \rightarrow D^{*+}D^- + c.c.$ cross section [1] are fitted by the χ^2 minimization method with different values for g_ψ . Panel (a) is obtained with $g_\psi = 1.73 \text{ GeV}^{-1}$, and panel (b) with $g_\psi = 0.52 \text{ GeV}^{-1}$. The dotted, dashed, short-dashed and short-dotted lines are for exclusive contributions from the light-vector mesons (LV), J/ψ , ψ' and $\psi(3770)$, respectively. In panel (a), the solid line represents the overall results, while the dash-dotted line if for exclusive contribution from $\psi(4040)$. In panel (b), the solid, dash-dot-dotted lines are for the overall results from two fitting schemes, i.e. Scheme-A and Scheme-B, respectively, while the dash-dotted and short-dash-dotted are for contributions from $\psi(4040)$ in these two schemes.

We can then extract the form-factor $|g_{\gamma^* D^{*+} D^-}|$ in the whole time-like region. In Fig. 3(a), we first look at the region around the $D^* \bar{D}$ threshold up to 5.0 GeV. As demonstrated by the solid line, the data can be described perfectly. We also include those two empirical fits presented in Ref. [7] as a comparison. The dashed line is generated by fitting the form factor data with an exponential function, i.e. with form factor one (FF-I):

$$\sqrt{2}g_{\gamma^* D^{*+} D^-}(s) = g_1 \exp[-(s - (m_D + m_{D^*})^2)/t_1] + g_0, \quad (21)$$

where $x = 0$ corresponds to the $D^* \bar{D} + c.c.$ threshold, and g_1 , t_1 , and g_0 are fitting parameters. The dotted line is given by fitting the data with a single resonance:

$$\sqrt{2}g_{\gamma^* D^{*+} D^-}(s) = \left| \frac{b_0}{s - m_X^2 + im_X \Gamma_X} + b_1 \right|, \quad (22)$$

with a background term b_1 . The parameter b_0 can be regarded as the product of the $\gamma^* X$ coupling and $XD\bar{D}^*$ coupling. This parametrization agrees with the data at higher energies, but drops at the threshold. In the above two equations, a factor $\sqrt{2}$ has been included for the change of conventions here. All the parameters have been given in Ref. [7].

In Fig. 4(a), we plot the \sqrt{s} -dependence of the form factor $g_{\gamma^* D^* \bar{D}}(s)$ for both charged and neutral channel in the whole time-like region up to 5.0 GeV. Since the coupling $g_{\psi^* D^* \bar{D}}$ (and $g_{J/\psi D^* \bar{D}}$) has the same value in these two channels, these two form factors converge to each other around the threshold region. In the low- \sqrt{s} region, the discrepancy arises from the total width difference between $D^{*\pm} \rightarrow D^\pm \gamma$ and $D^{*0} \rightarrow D^0 \gamma$. For the latter, the experimental data only give an upper limit, i.e. $\Gamma(D^{*0} \rightarrow D^0 \gamma) < 2.1$ MeV [3]. This corresponds to $|g_{\gamma D^{*0} D^0}(0)| < 11.3 \text{ GeV}^{-1}$, which has not been marked in the figure.

In Fig. 4(b), the form factor in the small \sqrt{s} region is plotted in association with its real and imaginary part. The resonance structures from $\rho(770)$, $\rho(1450)$ and $\rho(1700)$ are distinguishable. However, it should be cautioned that this kinematic region would suffer from a lack of information about the light vector meson couplings to $D^* \bar{D}$. Our model bridges the real photon form factor with the high- \sqrt{s} one, but inevitably leaves the middle range with large uncertainties. We drop the high- \sqrt{s} part between 2.5 GeV and 4.5 GeV since the structure of the real and imaginary part appears trivially as either very narrow peaks or very narrow dips.

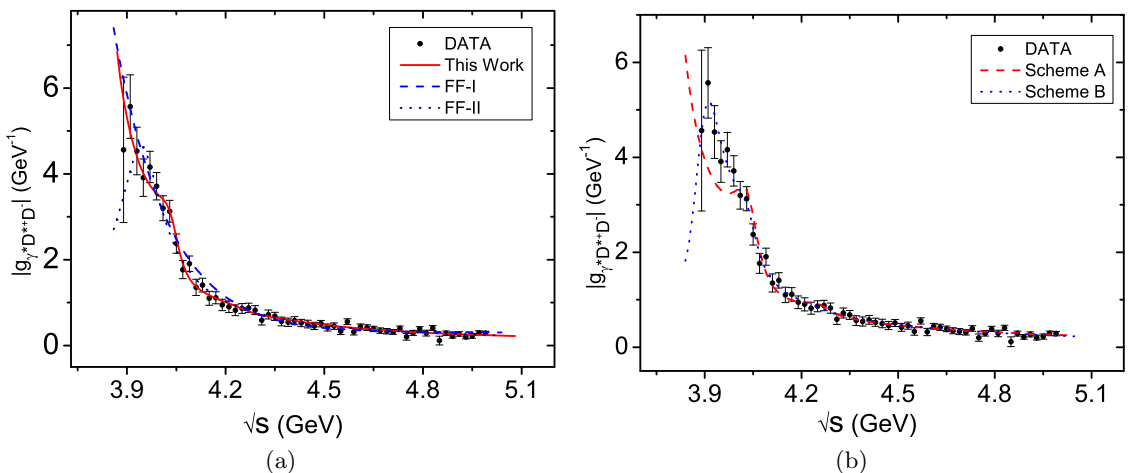


FIG. 3: The \sqrt{s} -dependence of form factor $|g_{\gamma^* D^{*+} D^-}(s)|$ extracted from the fitting results. In panel (a), the solid line is obtained from the fitting results with $g_\psi = 1.73 \text{ GeV}^{-1}$, while the dashed and dotted lines are for FF-I and FF-II results from Ref. [7]. In panel(b), the dashed and the dotted lines are obtained from the fitting results with $g_\psi = 0.52 \text{ GeV}^{-1}$ for Scheme-A and B, respectively.

The following points are advocated to understanding this fitting results:

(i) Numerically, the large contributions from ψ' are due to a relatively large g_ψ as shown by Eq. (12). In Ref. [7], we showed that the coupling $g_{\psi' D\bar{D}}$ can be well-constrained by the cross section lineshape of $e^+e^- \rightarrow D\bar{D}$. Thus, the coupling $g_{\psi' D^*\bar{D}}$ is actually enhanced by g_ψ via Eq. (12).

(ii) The relative phases appear to be sensitive to the cross section lineshape of $e^+e^- \rightarrow D^*\bar{D}$, and cancellations among the dominant amplitudes seem to be inevitable. Such interferences generally would affect the extraction of resonance parameters. Because of this, it is desirable to have a precise measurement of the lineshape of $e^+e^- \rightarrow D^*\bar{D} + c.c.$

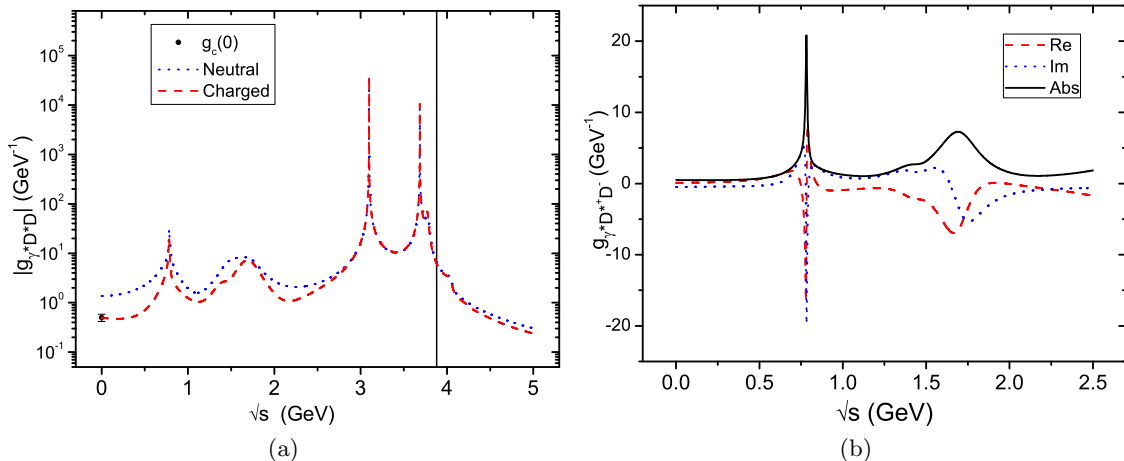


FIG. 4: The \sqrt{s} -dependence of form factor $|g_{\gamma^* D^* \bar{D}}(s)|$ extracted from the fitting results with $g_\psi = 1.73 \text{ GeV}^{-1}$. In panel (a), the dashed and dotted line stand for the form factors for the charged and neutral channel, respectively. In panel (b), the solid line is the form factor $|g_{\gamma^* D^* \bar{D}}(s)|$ for the charged channel, while the dashed and dotted line denote respectively the real and imaginary part of $g_{\gamma^* D^* \bar{D}}(s)$.

In order to clarify the interferences among the charmonium states, we identify the exclusive contributions from light vector mesons and charmonium states in $D^{*\pm} \rightarrow D^\pm \gamma$, where we expect that the light vector mesons should play a significant role. We first inspect the separated contributions to the partial width of $D^{*\pm} \rightarrow D^\pm \gamma$ from the light vector mesons and charmonia, and the results are as follows:

$$\begin{aligned} \Gamma_{LV}(D^{*\pm} \rightarrow D^\pm \gamma) &= 2.21 \text{ keV}, \\ \Gamma_\psi(D^{*\pm} \rightarrow D^\pm \gamma) &= 1.61 \text{ keV}, \end{aligned} \quad (23)$$

where Γ_{LV} and Γ_ψ are decay widths contributed by the light vector mesons, i.e. ρ, ω etc, and the charmonia, i.e. $J/\psi, \psi'$ etc. Interestingly, it shows that, although the light vector mesons play a dominant role, contributions from the charmonium states are still sizeable. In comparison with the experimental result $\Gamma(D^{*\pm} \rightarrow D^\pm \gamma) = 1.54 \text{ keV}$ [3], one can see that a destructive interference between these two components is required.

Such destructive phases are also present within the charmonium states. As follows, we list the exclusive contributions from $J/\psi, \psi'$, and $\psi(3770)$:

$$\begin{aligned} \Gamma_{J/\psi}(D^{*\pm} \rightarrow D^\pm \gamma) &= 8.07 \text{ keV}, \\ \Gamma_{\psi'}(D^{*\pm} \rightarrow D^\pm \gamma) &= 5.11 \text{ keV}, \\ \Gamma_{\psi(3770)}(D^{*\pm} \rightarrow D^\pm \gamma) &= 0.93 \text{ keV}. \end{aligned} \quad (24)$$

Other charmonium exclusive contributions are negligibly small. So we do not list them here.

B. With smaller g_ψ by heavy quark theory

As pointed out earlier, the relatively large contributions from the charmonium states, in particular, J/ψ and ψ' , are mainly due to the larger value of g_ψ in comparison with those given by the heavy quark theory [8] and the relativistic potential model [9]. In order to examine the impact from a possible overestimate of the coupling g_ψ due to the experimental uncertainties [3], we perform another fit of the $e^+e^- \rightarrow D^{*+}D^- + c.c.$ cross sections adopting $g_\psi = 0.52 \text{ GeV}^{-1}$ [8].

Two fitting schemes are considered. In Scheme-A, we fix $g_\psi = 0.52 \text{ GeV}^{-1}$ and fit the data with the same parameters. The fitted parameters are listed in Table IV. Relatively large χ^2 is found and the fit cannot account for the cross section lineshape near threshold as shown by the solid line in Fig. 3(b). The major deviations occur near threshold where a cross section deficit is revealed. The relatively small g_ψ also leads to suppressed contributions from J/ψ , ψ' and $\psi(3770)$. In contrast with the fitting of Subsection III A, this scheme requires constructive phases among the charmonium amplitudes.

In Scheme-B, we still fix $g_\psi = 0.52 \text{ GeV}^{-1}$, and introduce contributions from an additional resonance $X(3900)$ in order to overcome the cross section deficit near threshold. When we introduce the $X(3900)$ resonance, it is difficult to obtain the fitting solution if we leave the resonance parameters free, i.e. the mass and total width. We then take $m_X = 3.9 \text{ GeV}$ and $\Gamma_X = 89.8 \text{ MeV}$, which were extracted from $e^+e^- \rightarrow D\bar{D}$ in Ref. [7], as an input. The other fitted parameters are listed in Table IV, and relatively smaller χ^2 is found. In Fig. 2(b), the results for Scheme-A and B are compared with each other. It shows that contributions from the $\psi(4040)$ are relatively suppressed due to the presence of the $X(3900)$. Some interfering effects for the $Y(4260)$ are also observed in Scheme-A, but not in Scheme-B. As shown in Table IV, the combined coupling for the $Y(4260)$ still has large uncertainties.

TABLE III: Model parameters obtained from the χ^2 minimization fitting with $g_\psi = 0.52 \text{ GeV}^{-1}$. We fix $m_X = 3.9 \text{ GeV}$ and $\Gamma_X = 89.8 \text{ MeV}$, which are from Ref. [7]. The phase angles are in radian.

parameter	ϕ_{LV}	$\phi_{\psi'}$	$\phi_{\psi(3770)}$	$\phi_{\psi(4040)}$	$g_{\psi(4040)}^{\text{eff}}$	$g_{Y(4260)}^{\text{eff}}$	$g_{X(3900)}^{\text{eff}}$	$\phi_{X(3900)}$	$\chi^2/\text{d.o.f}$
Scheme A	5.72 ± 0.63	3.56 ± 0.10	3.69 ± 0.22	0.0 ± 0.11	0.58 ± 0.05	0.08 ± 0.03	-	-	63.9/51
Scheme B	5.69 ± 0.66	4.21 ± 0.43	2.23 ± 0.35	5.62 ± 0.27	0.35 ± 0.07	0.01 ± 0.04	1.89 ± 0.44	3.03 ± 0.26	38.8/49

In Fig. 3(b), the form factors extracted from Scheme-A and B are compared with the data. Again, we see that a smaller value for g_ψ cannot account for the form factor near threshold. Although the inclusion of an additional resonance $X(3900)$ can optimize the description, the form factor appears to drop quickly in the subthreshold region. This will lead to different trends of the form factor in the middle range of kinematics, i.e. \sqrt{s} is between $2 \sim 3.9 \text{ GeV}$.

The results with a smaller value for g_ψ seem to be different from those with a larger value. The following points can be learned and conjectured:

i) The resonance parameters extracted from the cross sections would contain uncertainties inevitably due to the uncertainty with g_ψ .

ii) The need of $X(3900)$ with a small g_ψ would bring questions on the underlying physics. On the one hand, if such a resonance indeed exists, problem will arise from how to organize it within the quark model framework. The systematic study of quark potential model seems not to have a place for this state below 4.2 GeV [16].

iii) To void the conflicts with the quark model, one possibility for such a structure would be due to the open channel effects of $D_s^*\bar{D}_s + c.c.$ Its threshold is 4.08 GeV , which is not far away from the $D^*\bar{D} + c.c.$ threshold. The final state interaction $D_s^*\bar{D} \rightarrow D\bar{D}^*$ via kaon exchange can produce a resonance-like enhancement near threshold. This is similar to the mechanism discussed in Ref. [7]. Also, justification of such a possibility would need the data for $e^+e^- \rightarrow D_s^*\bar{D}_s + c.c.$, which unfortunately are unavailable.

iv) As a comparison with the results from Subsection III A, we also list the exclusive contributions of the charmonium components to the radiative width in Table IV. Again, we see that with the smaller g_ψ , the charmonium contributions are also strongly suppressed in the real photon form factor. Nevertheless, a destructive phase exists between the J/ψ and ψ' amplitudes. Note that the contributions from the light vector mesons are unchanged.

TABLE IV: Exclusive contributions to the $D^{*\pm} \rightarrow D^\pm \gamma$ partial width from individual charmonium states with $g_\psi = 0.52 \text{ GeV}^{-1}$. Γ_ψ is the width given by a coherent sum of all the charmonium amplitudes.

Partial width (keV)	$\Gamma_{J/\psi}$	$\Gamma_{\psi'}$	$\Gamma_{\psi(3770)}$	$\Gamma_{\psi(4040)}$	Γ_ψ
Scheme-A	0.72	0.46	0.08	0.01	0.19
Scheme-B	0.72	0.46	0.08	0.00	0.31

C. Predictions for $D^* \rightarrow De^+e^-$

The ambiguity with the charmonium couplings will not affect the calculations for $D^* \rightarrow De^+e^-$ as long as the radiative decay $D^* \rightarrow D\gamma$ is fixed. This is simply because the mass of the electron (positron) is very small, and \sqrt{s} of the virtual photon is close to the real photon limit.

With the form factor determined in Subsection III A, we can predict the partial decay width of $D^* \rightarrow De^+e^-$ with the help of Eq. (16):

$$\Gamma(D^{*\pm} \rightarrow D^\pm e^+e^-) = 9.95 \text{ eV}. \quad (25)$$

It corresponds to a branching ratio, $BR(D^{*\pm} \rightarrow D^\pm e^+e^-) = 1.04 \times 10^{-4}$, and should be accessible in experiment, e.g. at BES-III [17]. This decay channel may provide some further constraints on the role played by the light vector mesons and charmonium states.

IV. SUMMARY AND DISCUSSION

In this work, we study the $D^* \bar{D} + c.c.$ production in e^+e^- annihilation from the threshold to $\sqrt{s} \simeq 5.0$ GeV in the VMD model. The recent experimental data from Belle [1] allow us to extract the form factor $g_{\gamma^* D^* \bar{D}}(s)$ in the time-like region.

Due to the uncertainties with the charmonium couplings to $D^* \bar{D} + c.c.$, we find two different solutions in the interpretation of the experimental data: i) With a relatively large coupling for $\psi D^* \bar{D}$, significantly large contributions from individual charmonium states are found. Destructive interferences among those charmonium components are hence required to bring down the overall cross sections, and then account for the cross section lineshape. ii) With a relatively small value for the $\psi D^* \bar{D}$ coupling, i.e. $g_\psi = 0.52 \text{ GeV}^{-1}$ [8], we find an apparent cross section deficit near threshold, and contributions from other mechanisms are needed.

We also try to fit the $e^+e^- \rightarrow D^{*+}D^- + c.c.$ with $g_\psi = 0.69 \text{ GeV}^{-1}$, which is obtained by QCD sum rules [12]. It shows that a cross section deficit still exists near threshold, although it becomes smaller than that with $g_\psi = 0.52 \text{ GeV}^{-1}$, and $\chi^2/\text{d.o.f} = 54.6/51$ is found. This suggests that a better fit of the near-threshold cross section would require a relatively large value for g_ψ . The consequence, however, is that destructive interferences among the resonances beyond the threshold region would be expected. In case that g_ψ has a relatively small value, such a cross section deficit, on the one hand, might imply the presence of an additional resonance $X(3900)$. On the other hand, we point out that an enhancement like that could be produced by the $D_s^* \bar{D}_s + c.c.$ open channel effects, and further experimental data will be able to clarify this issue.

In Ref. [7], $g_{\gamma^* D^{*+} D^-}(s)$ is extracted by two simple functions from which the behavior of the form factor below the $D^* \bar{D}$ threshold is, in principle, unknown. In this work, our model provides a description of the form factor $g_{\gamma^* D^* \bar{D}}(s)$ in the interplay region between the real photon energy and $D^* \bar{D}$ threshold, and some insights into the evolution of the vector meson contributions can be gained. Since this is a kinematic region which cannot be directly accessed by experiment, we expect further investigation of alternative processes would provide a test of our model, and more information on the underlying dynamics could be extracted. In particular, the partial decay width for $D^* \rightarrow De^+e^-$ is predicted in this framework. With a branching ratio of $BR(D^{*\pm} \rightarrow D^\pm e^+e^-) = 1.04 \times 10^{-4}$, this channel can be measured by BES-III in experiment. Our results also support such an idea that the enhancement around 3.9 GeV in $e^+e^- \rightarrow D\bar{D}$ [18] is caused by the open $D^* \bar{D}$ threshold effects [7].

It is worth mentioning a recent study of multiple solutions in extracting physics information from experiment [19]. Since it is not possible that all the numerical solutions are correct, a conjecture of selecting the physical solution is that the physical solution would correspond to the minimal magnitudes of the amplitudes. Further theoretical investigation of the $\psi D^* \bar{D}$ couplings and experimental information for $e^+e^- \rightarrow D_s^* \bar{D}_s + c.c.$ may help disentangle the underlying mechanism and also test the idea of Ref. [19].

Acknowledgement

We would like to thank G. Pakhlova, C.Z. Yuan and X.L. Wang for useful discussions regarding the Belle results. This work is supported, in part, by the National Natural Science Foundation of China (Grants No. 10675131), Chinese Academy of Sciences (KJCX3-SYW-N2), and Ministry of Science and Technology of China (2009CB825200).

-
- [1] K. Abe *et al.* [Belle Collaboration], Phys. Rev. Lett. **98**, 092001 (2007) [arXiv:hep-ex/0608018].
 - [2] B. Aubert *et al.* [BABAR Collaboration], Phys. Rev. D **79**, 092001 (2009) [arXiv:0903.1597 [hep-ex]].
 - [3] C. Amsler *et al.* [Particle Data Group], Phys. Lett. B **667**, 1 (2008).
 - [4] T. H. Bauer, R. D. Spital, D. R. Yennie and F. M. Pipkin, Rev. Mod. Phys. **50**, 261 (1978) [Erratum-ibid. **51**, 407 (1979)].
 - [5] T. Bauer and D. R. Yennie, Phys. Lett. B **60**, 169 (1976).
 - [6] T. M. Aliev, E. Iltan, N. K. Pak and M. P. Rekalov, Z. Phys. C **64**, 683 (1994).
 - [7] Y. J. Zhang and Q. Zhao, Phys. Rev. D **81**, 034011 (2010) [arXiv:0911.5651 [hep-ph]].
 - [8] A. Deandrea, G. Nardulli and A. D. Polosa, Phys. Rev. D **68**, 034002 (2003) [arXiv:hep-ph/0302273].
 - [9] P. Colangelo, F. De Fazio and G. Nardulli, Phys. Lett. B **334**, 175 (1994) [arXiv:hep-ph/9406320].
 - [10] R. Casalbuoni, A. Deandrea, N. Di Bartolomeo, R. Gatto, F. Feruglio and G. Nardulli, Phys. Rept. **281**, 145 (1997) [arXiv:hep-ph/9605342].
 - [11] Y. s. Oh, T. Song and S. H. Lee, Phys. Rev. C **63**, 034901 (2001) [arXiv:nucl-th/0010064].
 - [12] R. D. Matheus, F. S. Navarra, M. Nielsen and R. Rodrigues da Silva, arXiv:hep-ph/0310280.
 - [13] Y. Oh, W. Liu and C. M. Ko, Phys. Rev. C **75**, 064903 (2007) [arXiv:nucl-th/0702077].
 - [14] H. Y. Cheng, C. K. Chua and A. Soni, Phys. Rev. D **71**, 014030 (2005) [arXiv:hep-ph/0409317].
 - [15] T. M. Yan, H. Y. Cheng, C. Y. Cheung, G. L. Lin, Y. C. Lin, and H. L. Yu, Phys. Rev. D **46**, 1148 (1992); **55**, 5851(E) (1997); M. B. Wise, Phys. Rev. D **45**, R2188 (1992); G. Burdman and J. Donoghue, Phys. Lett. B **280**, 287 (1992).
 - [16] T. Barnes, S. Godfrey and E. S. Swanson, Phys. Rev. D **72**, 054026 (2005) [arXiv:hep-ph/0505002].
 - [17] D. M. Asner *et al.*, "Physics at BES-III, Edited by K.T. Chao and Y.F. Wang, Int. J. of Mod. Phys. **A 24** Supplement 1, (2009) [arXiv:0809.1869].
 - [18] G. Pakhlova *et al.* [Belle Collaboration], Phys. Rev. D **77**, 011103 (2008) [arXiv:0708.0082 [hep-ex]].
 - [19] C. Z. Yuan, X. H. Mo and P. Wang, arXiv:0911.4791 [hep-ph].